Anomalous evolution of Ar metastable density with electron density in high density Ar discharge

Min Park,[1] Hong-Young Chang,[1] Shin-Jae You,[2,a)] Jung-Hyung Kim,[2] and Yong-Hyeon Shin
[1]*Department of Physics, Korea Advanced Institute of Science and Technology, Daejeon 305-701, Korea*
[2]*Center for Vacuum Technology, Korea Research Institute of Standards and Science, Daejeon, 305-306 Korea*

(Received 22 March 2011; accepted 18 August 2011; published online 19 October 2011)

Recently, an anomalous evolution of argon metastable density with plasma discharge power (electron density) was reported [A. M. Daltrini, S. A. Moshkalev, T. J. Morgan, R. B. Piejak, and W. G. Graham, Appl. Phys. Lett. **92**, 061504 (2008)]. Although the importance of the metastable atom and its density has been reported in a lot of literature, however, a basic physics behind the anomalous evolution of metastable density has not been clearly understood yet. In this study, we investigated a simple global model to elucidate the underlying physics of the anomalous evolution of argon metastable density with the electron density. On the basis of the proposed simple model, we reproduced the anomalous evolution of the metastable density and disclosed the detailed physics for the anomalous result. Drastic changes of dominant mechanisms for the population and depopulation processes of Ar metastable atoms with electron density, which take place even in relatively low electron density regime, is the clue to understand the result. © *2011 American Institute of Physics*. [doi:10.1063/1.3640518]

I. INTRODUCTION

The energy levels from which electric dipole radiation is forbidden are called *metastable*.[1] An atom or molecule in metastable state can have much longer life-time than typical excited species which decay via electric dipole radiation.[2–4] Moreover, metastable levels are highly excited above the ground state so that metastable species can act as an energy reservoir. Because of these unusual properties, metastable species have been an interest in various fields such as geophysics, gas discharge lasers, and material processing plasmas.[5–7] In particular, in high density plasmas indispensable for modern semiconductor and display industries, metastable species play a crucial role in the plasma properties because the metastable species exist in a large fraction of the ground state atoms and thus, reactions concerned with metastables such as penning ionization and metastable pooling can occur appreciably. Hence, metastables have a considerable effect on the electron energy distribution function (EEDF) which is one of the most important parameters in plasmas.[8–11] In addition, the multistep ionization through the metastable state is known to be a dominant sustaining mechanism in high density discharges.[12–14]

There have been a number of experiments and theoretical calculations especially on argon atom metastable states ($1s_3$ and $1s_5$ in Paschen notation) density with regard to plasma power or pressure. In experiments, various techniques such as laser induced fluorescence (LIF),[15–18] laser absorption spectroscopy (LAS),[16,19–25] and optical emission spectroscopy (OES) (Refs. 26–29) were used to measure 1D or 2D distribution of metastable density. In theoretical research, by using various computational modelings such as collisional-radiative (CR) model or global model, 1D particle-in-cell (PIC) with Monte Carlo collisions (MCC), fluid model or hybrid Monte Carlo fluid model, extensive investigations have been conducted.[30–37] Recently, Daltrini *et al.*[38] and Graham *et al.*[39] reported a striking result that during the mode transition of inductively coupled plasma (ICP) discharge, there is a change of metastable density trend with plasma discharge power. In E-mode, the metastable density increases as the plasma power increases; however, it starts to decrease when the discharge is in H-mode. This anomalous evolution of metastable density with plasma discharge power has never been reported before. For example, Hebner and Miller[17] measured a slightly decreasing metastable density by LIF as the power increases in Ar ICP and suggested that it is due to the reduction in gas density by gas heating. However, Graham *et al.* mentioned that the decrease of the metastable density with power in H-mode of ICP in their experiment does not seem to be attributed to gas heating through measuring the rotational temperature of a trace amount of N_2. Tadokoro *et al.*[21] also measured 2D metastable density distribution in Ar ICP by LAS and suggested that the increase of the power does not necessarily increase the metastable density considering the electron induced quenching. Recently, Zhao and Wang[11] reported that the measured trend of metastable density by Daltrini *et al.* can be understood as a result of the spatial distribution change. Using the MC/fluid model where diffusion dominated metastable equation is inserted, they obtained 2D metastable density distributions in various conditions. When plasma power (or coil current) increases during the E-mode, metastable density increases with the maximum peak located in the center of discharge; however, in H-mode, the maximum peak of metastable density moves to the region close to the ICP antenna, therefore, at a fixed measurement point metastable density can seem to be anomalous. This suggestion is quite clear but limited to diffusion dominated metastable condition. On the other hand, Park *et al.*[40] suggested that the anomalous

a)Electronic mail: sjyou@kriss.re.kr.

evolution of metastable density can be due to the evolution of the EEDF during the mode transition. Changes in temperatures and densities of two different energy groups of electrons, accompanied by the EEDF evolution from a bi-Maxwellian to a Maxwellian during the mode transition, can affect the metastable density behavior. This is valid only in the case of non-local electron kinetic regime, and the calculation was done by inserting the experimentally measured parameters, not by self-consistent manner. In fact, the metastable density behavior with electron density (plasma power) remains not fully understood due to the absence of basic underlying physics, even though its importance cannot be overemphasized. In most cases in various processing plasmas, electron density is a typical internal parameter which can be controlled by adjusting radio frequency (RF) supply power. If we understand the relation between electron density and metastable density, it may provide us another control knob of discharge property and possibility leading to advanced plasma discharges for the future processing.

In this study, to establish basic physics of metastable density behavior with electron density, a simple global model presented by Lee and Chung[37] is used to calculate argon excited states densities (metastable state (4s), resonant state (4s), and 4p excited state). By solving three steady-state balance equations for metastable state (n_m), resonant state (n_r) and 4p state (n_p), we can obtain expressions for n_m, n_r and n_p as a function of electron density and electron temperature. From the particle balance equation, electron temperature is obtained by inserting electron density as an input parameter. Obtained electron temperature can be inserted into equations for n_m, n_r and n_p and then, three excited states density behaviors with electron density are obtained. The obtained n_m exhibits an anomalous evolution with electron density which agrees well with the experimental result in previous literature.[38,39] Drastic changes of dominant mechanisms for the population and depopulation processes of Ar metastable atoms with electron density, which takes place even in relatively low electron density regime, is the clue to understand the result.

II. MODEL

Modified particle and power balance equations including multi-step ionization in argon ICP discharge were derived and solved in a self-consistent manner by Lee and Chung.[37] In this paper, equations presented by Lee and Chung are replenished by finding missing terms which will be underlined in the expression.

The particle balance equations of each excited state are as follows:

$$\frac{dn_m}{dt} = K_{gm}n_e n_g + K_{rm}n_e n_r + (K_{pm}n_e + A_{pm,eff})n_p - \left[(K_{mr} + K_{mp} + K_{mg} + K_{mi})n_e + \frac{D_{eff}}{\Lambda^2}\right]n_m = 0, \quad (1)$$

$$\frac{dn_r}{dt} = K_{gr}n_e n_g + K_{mr}n_e n_m + (K_{pr}n_e + A_{pr,eff})n_p - \left[(K_{rp} + K_{rm} + K_{rg} + K_{ri})n_e + A_{r,eff} + \frac{D_{eff}}{\Lambda^2}\right]n_r = 0, \quad (2)$$

$$\frac{dn_p}{dt} = K_{gp}n_e n_g + K_{mp}n_e n_m + K_{rp}n_e n_r - \left[(K_{pm} + K_{pr} + K_{pg} + K_{pi})n_e + A_{pm,eff} + A_{pr,eff} + \frac{D_{eff}}{\Lambda^2}\right]n_p = 0, \quad (3)$$

where n_m is 4s metastable state density, n_r is 4s resonant state density, and n_p is 4p state density. K_{jk}'s are the rate constants of processes from j state to k state by electron impact, where j and k can be g, i, m, r, and p corresponding to ground state, ionized state, metastable state, resonant state, and 4p excited state, respectively. D_{eff} is the effective diffusion coefficient and Λ is the effective diffusion length given by

$$\frac{1}{\Lambda^2} = \left(\frac{\pi}{L}\right)^2 + \left(\frac{\chi_{01}}{R}\right)^2.$$

Here, $\chi_{01} \approx 2.405$ is the first zero of the zero-order Bessel function. $A_{pm,eff}$, $A_{pr,eff}$ and $A_{rg,eff}$ are effective radiative decay rates from 4p state to metastable state, 4p state to resonant state, and resonant state to ground state. These are calculated according to the model of Ashida *et al.*[41] considering the reabsorption of optical emission. All other rate coefficients and effective diffusion loss rate (D_{eff}) are listed in Table I and also followed from Lee and Chung.[42] Above three equations consist of a linear system in three variables n_m, n_r and n_p assuming other coefficients as symbolic constants then n_m, n_r and n_p can be calculated as follows:

TABLE I. Reactions and corresponding rate constants used in calculations (Ref. 42). Unit of K is $m^3\ s^{-1}$ and A is s^{-1}.

Reaction	Rate constant
$Ar + e \rightarrow Ar^+ + 2e$	$K_{gi} = 2.3 \times 10^{-14} T_e^{0.68} \exp(-15.76/T_e)$
$Ar_m + e \rightarrow Ar^+ + 2e$	$K_{mi} = 6.8 \times 10^{-15} T_e^{0.67} \exp(-4.2/T_e)$
$Ar_r + e \rightarrow Ar^+ + 2e$	$K_{ri} = 6.8 \times 10^{-15} T_e^{0.67} \exp(-4.2/T_e)$
$Ar_p + e \rightarrow Ar^+ + 2e$	$K_{pi} = 1.8 \times 10^{-13} T_e^{0.61} \exp(-2.61/T_e)$
$Ar + e \rightarrow Ar_m + e$	$K_{gm} = 2.5 \times 10^{-15} T_e^{0.74} \exp(-11.56/T_e)$
$Ar + e \rightarrow Ar_r + e$	$K_{gr} = 2.5 \times 10^{-15} T_e^{0.74} \exp(-11.56/T_e)$
$Ar + e \rightarrow Ar_p + e$	$K_{gp} = 1.4 \times 10^{-14} T_e^{0.71} \exp(-13.2/T_e)$
$Ar_m + e \rightarrow Ar + e$	$K_{mg} = 4.3 \times 10^{-16} T_e^{0.74}$
$Ar_r + e \rightarrow Ar + e$	$K_{rg} = 4.3 \times 10^{-16} T_e^{0.74}$
$Ar_p + e \rightarrow Ar + e$	$K_{pg} = 3.9 \times 10^{-16} T_e^{0.71}$
$Ar_m + e \rightarrow Ar_r + e$	$K_{mr} = 2.0 \times 10^{-13}$
$Ar_m + e \rightarrow Ar_p + e$	$K_{mp} = 8.9 \times 10^{-13} T_e^{0.51} \exp(-1.59/T_e)$
$Ar_r + e \rightarrow Ar_p + e$	$K_{rp} = 8.9 \times 10^{-13} T_e^{0.51} \exp(-1.59/T_e)$
$Ar_r + e \rightarrow Ar_m + e$	$K_{rm} = 3.0 \times 10^{-13}$
$Ar_p + e \rightarrow Ar_m + e$	$K_{pm} = 1.5 \times 10^{-13} T_e^{0.51}$
$Ar_p + e \rightarrow Ar_r + e$	$K_{pr} = 1.5 \times 10^{-13} T_e^{0.51}$
$Ar_r \rightarrow Ar + h\nu$	$A_{rg,eff} = 5 \times 10^6$
$Ar_p \rightarrow Ar_m + h\nu$	$A_{pm,eff} = 3 \times 10^4$
$Ar_p \rightarrow Ar_r + h\nu$	$A_{pr,eff} = 3 \times 10^4$
$D_{eff} \times n_g$[a]	$1.0 \times 10^{20}\ (m^{-1}s^{-1})$

[a] n_g is atom density of ground state in m^{-3}.

$$n_m = \frac{1}{\alpha}\Big[(bcK_{gm} + \underline{bK_{gp}A_{pm}})n_e + (bK_{gp}K_{pm} + cK_{gr}K_{rm} + \underline{K_{gr}K_{rp}A_{pm} + K_{gp}K_{rm}A_{pr} - K_{gm}K_{rp}A_{pr}})n_e^2 + (K_{gp}K_{pr}K_{rm} + K_{gr}K_{rp}K_{pm} - K_{gm}K_{pr}K_{rp})n_e^3\Big]n_g, \quad (4)$$

$$n_r = \frac{1}{\alpha}\Big[(acK_{gr} + \underline{aK_{gp}A_{pr}})n_e + (cK_{gm}K_{mr} + aK_{gp}K_{pr} + \underline{K_{gm}K_{mp}A_{pr} + K_{gp}K_{mr}A_{pm} - K_{gr}K_{mp}A_{pm}})n_e^2 + (K_{gp}K_{pm}K_{mr} + K_{gm}K_{mp}K_{pr} - K_{gr}K_{mp}K_{pm})n_e^3\Big]n_g, \quad (5)$$

$$n_p = \frac{1}{\alpha}\Big[abK_{gp}n_e + (aK_{gr}K_{rp} + bK_{gm}K_{mp})n_e^2 + (K_{gr}K_{rm}K_{mp} + K_{gm}K_{mr}K_{rp} - K_{gp}K_{mr}K_{rm})n_e^3\Big]n_g, \quad (6)$$

where

$$a = (K_{mr} + K_{mp} + K_{mg} + K_{mi})n_e + \frac{D_{eff}}{\Lambda^2},$$

$$b = (K_{rp} + K_{rm} + K_{rg} + K_{ri})n_e + A_{rg,eff} + \frac{D_{eff}}{\Lambda^2},$$

$$c = (K_{pm} + K_{pr} + K_{pg} + K_{pi})n_e + A_{pm,eff} + A_{pr,eff} + \frac{D_{eff}}{\Lambda^2},$$

$$\alpha = abc - \underline{(aK_{rp}A_{pr,eff} + bK_{mp}A_{pm})n_e} - (aK_{pr}K_{rp} + bK_{mp}K_{pm} + cK_{mr}K_{rm} + \underline{K_{mp}K_{rm}A_{pr,eff} + K_{mr}K_{rp}A_{pm,eff}})n_e^2 - (K_{mp}K_{pr}K_{rm} + K_{mr}K_{rp}K_{pm})n_e^3.$$

The electron and ion fluxes to the wall are given by

$$\Gamma_e = \Gamma_i = n_s u_B. \quad (7)$$

Here, u_B is the Bohm velocity and n_s is the electron density at the plasma-sheath edge. Godyak.[43] has solved the diffusion equations analytically and obtained the analytical solutions for n_s and expressed as follows:

$$n_{s,l} \equiv n_e h_l, \quad n_{s,r} \equiv n_e h_r,$$

$$h_l \approx 0.86\left(3 + \frac{L}{2\lambda_i}\right)^{-1/2}, \quad (8)$$

$$h_r \approx 0.80\left(4 + \frac{R}{2\lambda_i}\right)^{-1/2}, \quad (9)$$

where $n_{s,l}$ and $n_{s,r}$ are electron densities at the axial and radial plasma-sheath edge. λ_i is the ion-neutral collision mean free path and given by $\lambda_i = (330p)^{-1}$ cm in argon at pressure p(mTorr).[1] The particle balance equation between the total volume ionization and the total surface ion loss is written as

$$\sum_i VK_{iz,i}n_i n_e = V(K_{gi}n_g + K_{mi}n_m + K_{ri}n_r + K_{pi}n_p)n_e = n_e u_B(A_l h_l + A_r h_r),$$

where $V = \pi R^2 L$ is the plasma volume and $A_l = 2\pi R^2$ and $A_r = 2\pi RL$ are sheath areas of axial and radial directions, respectively. In the calculation, the chamber size was assumed as $R = 8$ cm and $L = 4$ cm (as the same size as GECRC (Ref. 44)) and pressure was set at 50 mTorr.

III. RESULT AND DISCUSSION

Calculated densities of metastable state (n_m), resonant state (n_r), and 4p excited state (n_p) are shown in Fig. 1 as a function of electron density. Metastable state density n_m shows an anomalous evolution with electron density in low electron density regime, quite analogous to the previous experimental results.[38,39] On the other hand, resonant state density n_r and 4p excited state density n_p increase monotonically, also well agreed with previous experiments.[45,46]

Behavior of n_m can be understood from population (generation) and depopulation (loss) balance point of view. First, let us divide electron density range into three regimes with respect to the metastable density behavior with electron

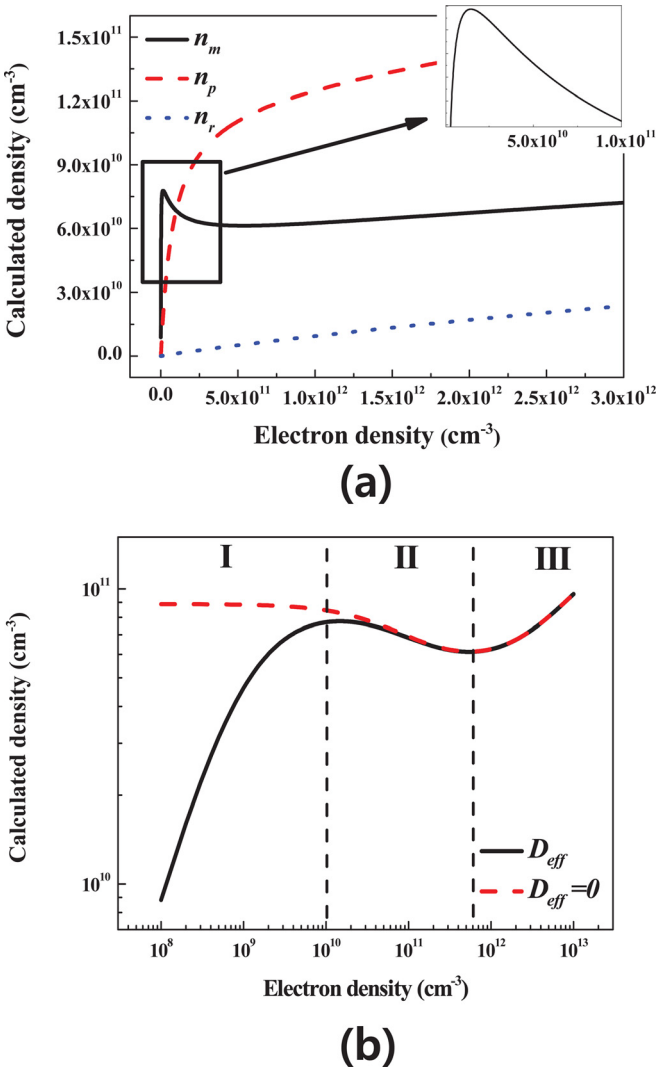

FIG. 1. (Color online) (a) Calculated metastable state density (n_m), resonant state density (n_r) and 4p state density (n_P) against electron density. (b) Metastable density with diffusive loss (solid line) and without diffusive loss (dashed line) against electron density in log scale. Electron density range is divided into three regimes with respect to behavior of metastable density.

density as shown in Fig. 1(b) and find out what are the dominant population and depopulation mechanisms for metastable state. Here, population and depopulation mechanisms can be classified as electron collisional or non-electron collisional one. Non-electron collisional means the processes occurring without electron collision such as radiative decay to lower level or diffusive loss to walls.

In the electron density range $n_e < 10^9$ cm^{-3} relevant to the beginning of regime (I), the dominant depopulation mechanism for n_m is diffusive loss to walls $\left(n_m \frac{D_{eff}}{\Lambda^2}\right)$ and the dominant population mechanism is, however, not distinguished between electron collisional and non-collisional (radiative) in Fig. 2. Electron collisional population mechanism indicates electron impact excitation from ground state $K_{gm} n_g n_e$, mixing from resonant state $K_{rm} n_r n_e$ and de-excitation from 4p state $K_{pm} n_p n_e$. Radiative population mechanism is radiative decay from 4p state $A_{pm,eff} n_p$. In this range, balance equation for n_m can be expressed as

$$n_m \frac{D_{eff}}{\Lambda^2} \simeq \left(K_{gm} n_g + K_{rm} n_r + K_{pm} n_p\right) n_e + A_{pm,eff} n_p. \quad (10)$$

The left and right sides of above equation correspond to depopulation and population rates, respectively. On the right side, electron collisional population rate $((K_{gm} n_g + K_{rm} n_r + K_{pm} n_p) n_e)$ obviously increases with increasing electron density because electron density n_e is directly multiplied in the expression. Of course, n_r and n_p as well as electron temperature implied in the rate coefficients (K_{gm}, K_{rm}, K_{pm}) can affect population rate; however, their variations are small that the overall trend with electron density is simply proportional to n_e. Non-electron collisional population rate ($A_{pm,eff} n_p$) also increases with electron density because $A_{pm,eff}$ is a constant value and n_p increases with electron density as shown in Fig. 1. Monotonically increasing behaviors of n_r and n_p with electron density will be discussed later. On the left side of Eq. (10), depopulation rate is simply expressed as the state density n_m multiplied by constant value $\frac{D_{eff}}{\Lambda^2}$. Therefore, in the beginning of regime (I), population rate (right side of Eq. (10)) increases with increasing electron density and then metastable density (left side of Eq. (10)) should increase to balance population and depopulation rates in the steady-state. In other words, n_m has an increasing behavior with electron density when $n_e < 10^9$ cm^{-3} because depopulation mechanism is non-electron collisional, thus proportional only to n_m itself. This argument can be double-checked by the calculation result assuming no diffusive loss ($D_{eff} = 0$). Fig. 1(b) shows that if there is no diffusive loss, increasing behavior of metastable density in regime (I) does not appear. It is noticeable that due to non-electron collisional depopulation mechanism (diffusive loss to walls), metastable density can exhibit increasing behavior with electron density in regime (I).

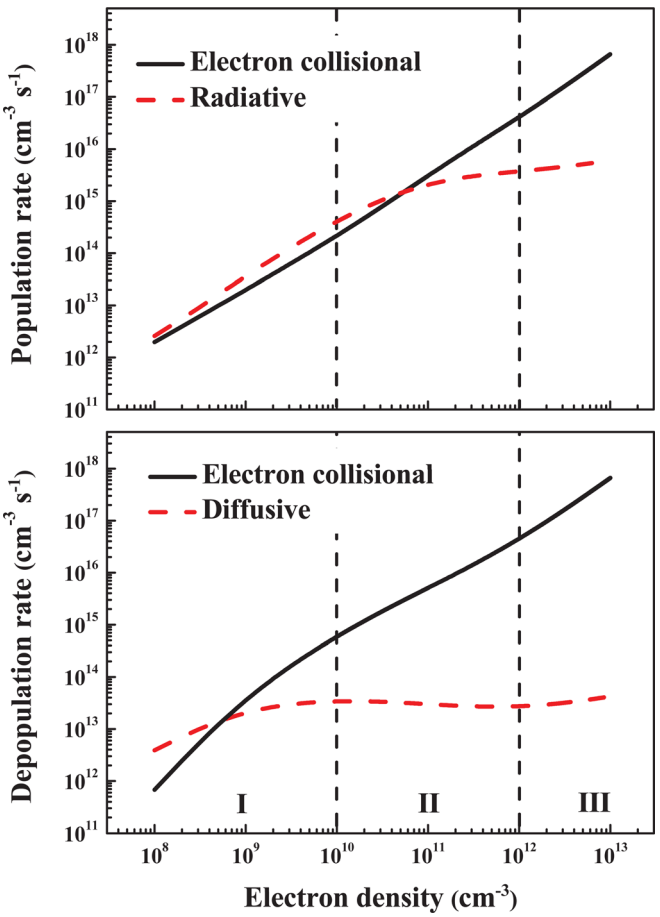

FIG. 2. (Color online) Population and depopulation rates for metastable state as a function of electron density, where electron collisional rate (solid line) and non-electron collisional rate (dashed line) are separated.

In regimes (II) and (III) of Fig. 1(b), calculated results with and without diffusive loss are not much different because in that range the dominant depopulation mechanism is electron collisional (Fig. 2). Thus, balance equation for n_m in this range can be expressed as follows ignoring diffusive loss:

$$n_m \left(K_{mr} + K_{mp} + K_{mg} + K_{mi}\right) n_e \simeq \left(K_{gm} n_g + K_{rm} n_r + K_{pm} n_p\right) n_e + A_{pm,eff} n_p. \quad (11)$$

Now, the dominant depopulation rate in the left side is electron collisional: electron impact mixing to 4s resonant state $K_{mr} n_m n_e$, excitation to 4p state $K_{mp} n_m n_e$, de-excitation to ground state $K_{mg} n_m n_e$, ionization $K_{mi} n_m n_e$. In this case, behavior of metastable density cannot be determined simply with the same manner as above because n_e is multiplied on the left side, i.e., electron collisional depopulation mechanism. Instead of Eq. (11), we can express n_m as follows:

$$n_m \simeq \frac{\left(K_{gm} n_g + K_{rm} n_r + K_{pm} n_p\right) n_e}{\left(K_{mr} + K_{mp} + K_{mg} + K_{mi}\right) n_e} + \frac{A_{pm,eff} n_p}{\left(K_{mr} + K_{mp} + K_{mg} + K_{mi}\right) n_e}. \quad (12)$$

Above equation is divided into two terms by the population mechanisms in the numerators: electron collisional (the first term) and non-electron collisional (the second term). We calculated two terms in Eq. (12) separately to see how they behave with electron density and contribute to behavior of metastable density (Fig. 3). It is found that the second term is the origin of decreasing behavior of metastable density in regime (II). The second term of Eq. (12) shows a drastic

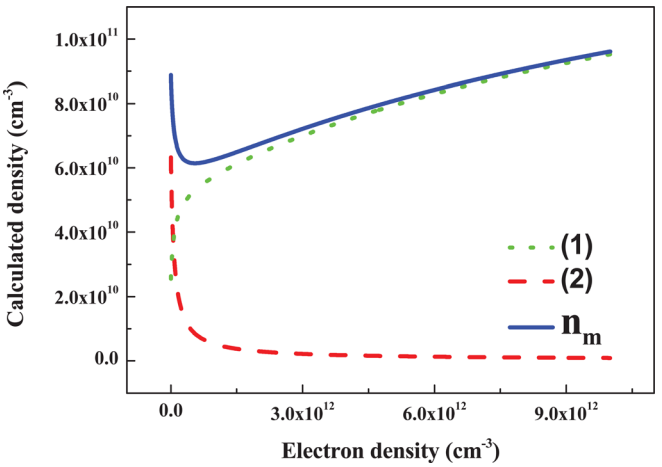

FIG. 3. (Color online) Metastable density (nm) when $n_e \geq 10^{10}$ cm^{-3} and each term of the Eq. (12) as a function of electron density, where (1) (dotted line) and (2) (dashed line) corresponding to the first and the second terms of Eq. (12), respectively.

decrease with electron density in Fig. 3, which is corresponding to the result of the balance between population from 4p state by radiative decay and depopulation by electron collision to ground state, 4p state, resonant state, and ionization, i.e., balance between non-electron collisional population mechanism and electron collisional depopulation mechanism. The second term in Eq. (12) can be approximated as

$$\frac{Cn_p}{\alpha n_e},$$

where C is constant corresponding to radiative decay rate constant from 4p state and α is an arbitrary function of electron temperature T_e. Then, it would follow the trend of $\frac{n_p}{n_e}$ assuming small T_e variation. In this case, however, we cannot expect how $\frac{n_p}{n_e}$ behaves with electron density only with the fact that n_p increases monotonically with electron density. Thus, we use the numerical fitting result $n_p \approx 6.58 \times 10^7 \times n_e^{0.268}$ obtained by numerical fitting based on a simple form of $a \times n_e^b$ where a and b are arbitrary fitting parameters. At this time, we adopt this result and will discuss later how n_p can be expressed in such a simple form. Then, $\frac{n_p}{n_e}$ follows the trend of $\frac{1}{n_e^{\chi}}$ where $\chi < 1$ and this term would decrease with electron density, and in fact, it shows decreasing behavior with electron density in Fig. 3. The decreasing behavior of metastable density with electron density in regime (II) results from the balance between non-electron collisional population and electron collisional depopulation.

The first term of Eq. (12), corresponding to the balance between electron collisional population and depopulation mechanisms, shows increasing behavior with electron density. In this term, n_e can be canceled out, then

$$\frac{\beta}{\alpha}n_g + \frac{\gamma}{\alpha}n_r + \frac{\delta}{\alpha}n_p,$$

where α, β, γ, and δ are arbitrary functions of electron temperature T_e. Because T_e does not change significantly, this follows the trends of n_r and n_p. Since we know that n_r and n_p increase with electron density from the calculation (Fig. 1(a)), this term exhibits increasing behavior with electron density as shown in Fig. 3. This term corresponds to the behavior of metastable density in regime (III). It is noticeable that because both population and depopulation mechanisms are electron collisional, metastable density can be simply understood and found to follow the behaviors of n_r and n_p.

In brief, anomalous evolution of metastable density with electron density is attributed to the combined effect of population and depopulation mechanisms. In particular, when population mechanism for metastable state is non-electron collisional and depopulation mechanism is electron collisional (regime (II)), metastable density can have a decreasing behavior with electron density. It is obvious that when non-electron collisional depopulation mechanism is dominant (regime (I)), metastable density increases with electron density. When population and depopulation mechanisms are both electron collisional, metastable density also increases with electron density (regime (III)).

Now, let us discuss the behavior of n_r and n_p with electron density. As mentioned above, monotonically increasing behaviors of n_r and n_p with electron density can be expressed as a simple form of $a \times n_e^b$ obtained by numerical fitting, where a and b are arbitrary fitting parameters. Let us see how n_r and n_p can be expressed in such a simple form. Fig. 4 shows calculated depopulation rates for each state. For n_r, radiative decay to ground state is the dominant depopulation mechanism in the whole electron density range (Fig. 4(a)). This is the same situation as metastable state when diffusive loss (non-electron collisional) is the dominant depopulation mechanism (regime (I)). That is, because population rate is only proportional to n_r itself, n_r should increase with increasing electron density to balance population and depopulation rates. Thus, resonant state density n_r exhibits monotonically increasing behavior in the whole electron density range. For n_p, radiative decay to metastable state and resonant state are the dominant depopulation mechanisms until $n_e \simeq 10^{11}$cm^{-3}. Above $n_e \simeq 10^{11}$cm^{-3}, the dominant depopulation mechanism is changed to electron collisional. However, for n_p, there is no non-collisional population mechanism. Both population and depopulation mechanisms are electron-collisional and thus, n_p again exhibits increasing behavior with electron density. In fact, there exists population mechanism from higher states by radiative decay; however, since their number densities would be very low, we can ignore its contribution. The transition of depopulation mechanism affects the increasing slope of n_p. In Fig. 1(a), we can see that above $n_e > 10^{11}$ cm^{-3} the increasing slope of n_p is decreased. Based on aforementioned argument, n_r and n_p can be expressed as follows:

$$n_r \simeq \frac{(K_{gr}n_g + K_{mr}n_m + K_{pr}n_p)n_e + A_{pr,eff}n_p}{A_{rg,eff}}. \quad (13)$$

When $n_e \leq 10^{11}$ cm^{-3},

$$n_p \simeq \frac{(K_{gp}n_g + K_{mp}n_m + K_{rp}n_r)n_e}{(A_{pm,eff} + A_{pm,eff})}. \quad (14)$$

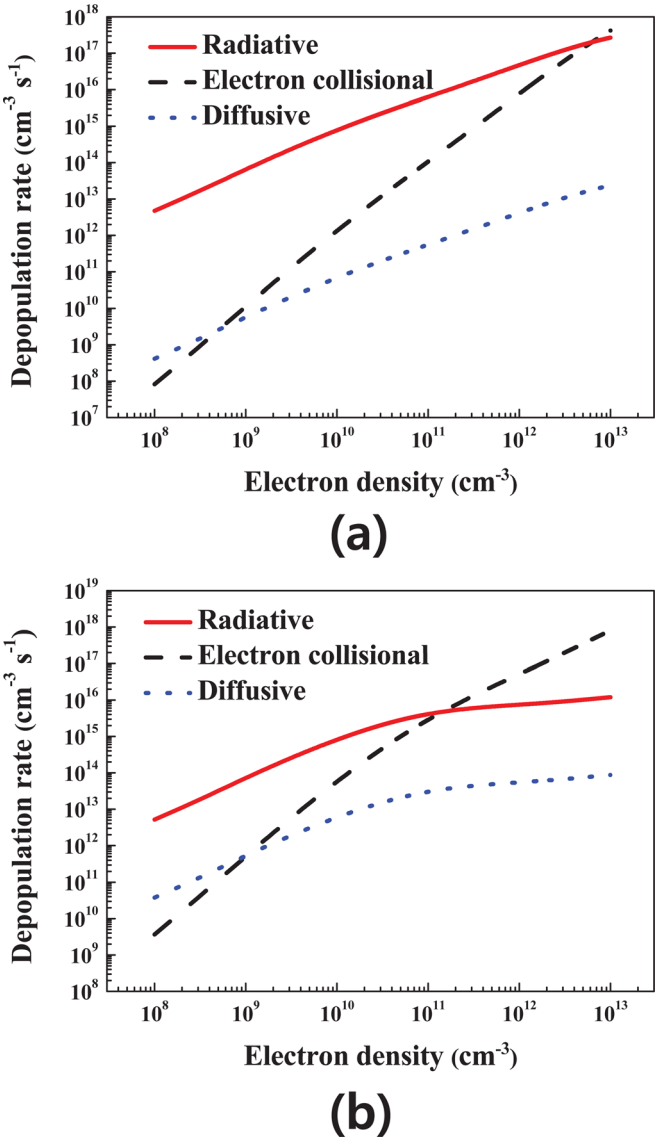

FIG. 4. (Color online) Depopulation rate for (a) resonant state (b) 4p state as a function of electron density.

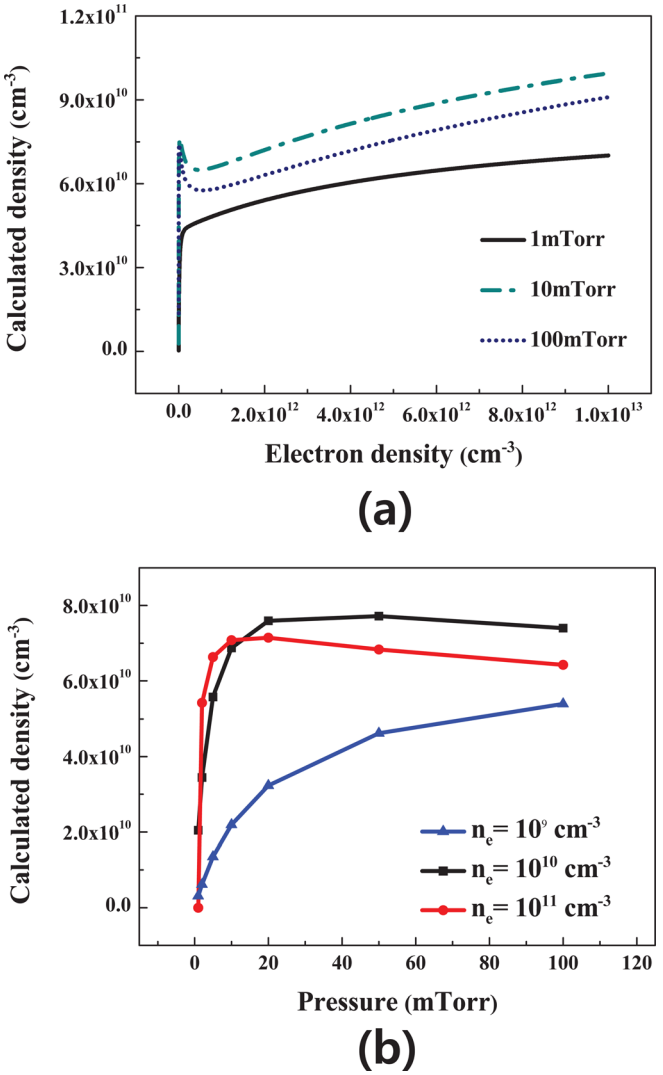

FIG. 5. (Color online) (a) Metastable density as a function of electron density at pressures 1 mTorr (solid line), 10 mTorr (dash-dotted line), 100 mTorr (dotted line). (b) Metastable density as a function of pressure at three fixed electron densities (10^9 cm^{-3}, 10^{10} cm^{-3}, 10^{11} cm^{-3}).

When $n_e \geq 10^{11}$ cm^{-3},

$$n_p \simeq \frac{(K_{gp}n_g + K_{mp}n_m + K_{rp}n_r)n_e}{(K_{pm} + K_{pr} + K_{pg} + K_{pi})n_e}. \quad (15)$$

Above equations can be simplified as a form of $a \times n_e^b$ as we assumed above. We suggest that density of ordinary state which can be depopulated by radiative decay exhibits monotonically increasing behavior with electron density.

As summarizing the above argument, when the electron density is below 10^{10} cm^{-3} (regime (I)), metastable density rapidly increases as the electron density increases due to the diffusive loss mechanism, then it starts to decrease (regime (II)) because the dominant depopulation mechanism is changed to electron collisional; but the dominant population mechanism is still a radiative process (non-electron collisional). When $n_e \geq 10^{12}$ cm^{-3} (regime (III)), both dominant depopulation and population mechanisms are electron collisional, and the metastable density increases following the behaviors of n_r and n_p. Due to its intrinsic characteristic–electric dipole radiation forbidden, the transition of depopulation mechanism from non-electron collisional to electron collisional occurs at relatively low electron density range, and metastable density can decrease with electron density above a certain electron density. In the case of ordinary excited states such as resonant state and 4p state, because they can be depopulated by radiative decay which is quite a strong non-electron collisional depopulation mechanism, the transition of depopulation mechanism occurs at high electron density range where population mechanism is already changed to electron collisional; thus, they exhibit monotonically increasing behavior with electron density.

Let us discuss briefly the possibility to control metastable density behavior. Figure 5(a) shows that metastable density behavior with electron density can be varied at different pressures. At low pressure, metastable density behavior is monotonic; however, as the pressure increases anomalous behavior of metastable density appears at low electron density regime.

This indicates that the pressure change affects the strength of diffusive loss mechanism and this can lead to the modification of metastable density behavior. It is noted that the offset of metastable density also exhibits anomalous behavior, suggested as due to the combined effect of electron density and temperature change. Figure 5(b) also indicates that if we fix the electron density, then the metastable density shows an anomalous behavior with the pressure above a certain electron density. At low electron density ($n_e = 10^9$ cm^{-3}), the dominant depopulation mechanism is diffusive loss to walls and increasing behavior of metastable density is observed as the pressure increases. However, at intermediate electron density ($n_e = 10^{10}$ cm^{-3}) and high electron density ($n_e = 10^{11}$ cm^{-3}), metastable density decreases after a certain pressure although their extent of change with pressure is different. In practice, plasma power can be fixed and electron density will be increased with increasing pressure and electron temperature also changes, so the metastable density behavior with pressure at a fixed power becomes rather complicated.[17,45] This may be understood based on electron density, but further investigation is needed.

IV. CONCLUSION

We investigated excited states argon atom densities via a simple global model. Calculated result indicates that metastable state density exhibits an anomalous evolution with the electron density; meanwhile, other excited states show monotonically increasing behaviors, which agrees well with the experimental result in previous literature. It is found that drastic changes of dominant mechanisms for the population and depopulation processes of Ar metastable atoms with electron density, which takes place even in relatively low electron density regime, are the clues to understand the result. We have also looked into the possibility to control metastable density behavior. It is suggested that pressure is also a key factor to control metastable density together with the power (electron density). Thorough understanding of metastable density behavior will provide us another control knob of plasma discharge for the next-generation processing.

ACKNOWLEDGMENTS

This research was supported by National R&D Program through the National Research Foundation of Korea (NRF) funded by the Ministry of Education, Science and Technology (2009-0082624). This work was also sponsored in part by the Korea Ministry of Knowledge Economy (10034836, 10031812-2008-11, 10034827, 2011K000828, 2011K000789, 2010T100100265).

[1]M. Lieberman and A. Lichtenberg, *Principles of Plasma Discharges and Materials Processing* 2nd ed. (Wiley, New York, 2005).
[2]E. Muschlitz, Jr., Science **159**, 599 (1968).
[3]H. Katori and F. Shimizu, Phys. Rev. Lett. **70**, 3545 (1993).
[4]G. Piech, J. Boffard, M. Gehrke, L. Anderson, and C. Lin, Phys. Rev. Lett. **81**, 309 (1998).
[5]J. Jacob and J. Mangano, Appl. Phys. Lett. **28**, 724 (1976).
[6]M. Torr and D. Torr, Rev. Geophys. **20**, 91, doi: 10.1029/RG020i001p00091 (1982).
[7]W. Lu, K. Baldwin, M. Hoogerland, S. Buckman, T. Senden, T. Sheridan, and R. Boswell, J. Vac. Sci. Technol. B **16**, 3846 (1998).
[8]N. Bassett and D. Economoua, J. Appl. Phys. **75**, 1931 (1994).
[9]L. Overzet and J. Kleber, Plasma Sources Sci. Technol. **7**, 512 (1998).
[10]M. Roberto, H. Smith, and J. Verboncoeur, IEEE Trans. Plasma. Sci. **31**, 1292 (2003).
[11]S. Zhao and Y. Wang, J. Phys. D: Appl. Phys. **43**, 275203 (2010).
[12]C. Ferreira, J. Loureiro, and A. Ricard, J. Appl. Phys. **57**, 82 (1985).
[13]T. Sato and T. Makabe, J. Appl. Phys. **98**, 113304 (2005).
[14]C. A. DeJoseph, Jr. and V. Demidov, J. Phys. B **38**, 3805 (2005).
[15]B. McMillin and M. Zachariah, J. Appl. Phys. **77**, 5538 (1995).
[16]G. Hebner, J. Appl. Phys. **80**, 2624 (1996).
[17]G. A. Hebner and P. A. Miller, J. Appl. Phys. **87**, 8304 (2000).
[18]G. Jackson, C. Lewis, S. Doorn, V. Majidi, and F. King, Spectrochim. Acta, Part B **56**, 2449 (2001).
[19]N. Beverini, G. Cicconi, G. Genovesi, and E. Piano, Plasma Sources Sci. Technol. **6**, 185 (1997).
[20]D. Leonhardt, C. Eddy, Jr., V. Shamamian, R. Fernsler, and J. Butler, J. Appl. Phys. **83**, 2971 (1998).
[21]M. Tadokoro, H. Hirata, N. Nakano, Z. L. Petrović, and T. Makabe, Phys. Rev. E **58**, 7823 (1998).
[22]E. Augustyniak, S. Filimonov, and J. Borysow, J. Appl. Phys. **86**, 4767 (1999).
[23]B. Bakowski, G. Hancock, R. Peverall, S. E. Prince, G. A. D. Ritchie, and L. J. Thornton, J. Phys. D: Appl. Phys. **38**, 2769 (2005).
[24]Y. Hayashi, S. Hirao, Y. Zhang, T. Gans, D. O'Connell, Z. Petrović, and T. Makabe, J. Phys. D: Appl. Phys. **42**, 145206 (2009).
[25]H. Do, V. Sushkov, and R. Hippler, New J. Phys. **11**, 033020 (2009).
[26]T. Czerwiec and D. B. Graves, J. Phys. D: Appl. Phys. **37**, 2827 (2004).
[27]D. Mariotti, Y. Shimizu, T. Sasaki, and N. Koshizaki, Appl. Phys. Lett. **89**, 201502 (2006).
[28]A. M. Daltrini, S. A. Moshkalev, M. J. R. Monteiro, E. Besseler, A. Kostryukov, and M. Machida, J. Appl. Phys. **101**, 073309 (2007).
[29]J. Boffard, R. Jung, C. Lin, and A. Wendt, Plasma Sources Sci. Technol. **18**, 035017 (2009).
[30]C. Braun and J. Kunc, Phys. Fluids **30**, 499 (1987).
[31]J. Vlcek and V. Pelikan, J. Phys. D: Appl. Phys. **24**, 309 (1991).
[32]D. P. Lymberopoulos and D. J. Economou, J. Appl. Phys. **73**, 3668 (1993).
[33]S. Rauf and M. J. Kushner, J. Appl. Phys. **82**, 2805 (1997).
[34]A. Bogaerts and R. Gijbels, Spectrochim. Acta, Part B **55**, 263 (2000).
[35]M. W. Kiehlbauch and D. B. Graves, J. Appl. Phys. **91**, 3539 (2002).
[36]L. Lauro-Taroni, M. Turner, and N. Braithwaite, J. Phys. D: Appl. Phys. **37**, 2216 (2004).
[37]M. H. Lee and C. W. Chung, Appl. Phys. Lett. **87**, 131502 (2005a).
[38]A. M. Daltrini, S. A. Moshkalev, T. J. Morgan, R. B. Piejak, and W. G. Graham, Appl. Phys. Lett. **92**, 061504 (2008).
[39]W. G. Graham, R. B. Piejak, T. J. Morgan, A. M. Daltrini, and S. A. Moshkalev, 19th Europhysics Conference on the Atomic and Molecular Physics of Ionized Gases, Granada, Spain, 2008.
[40]M. Park, H. Chang, S. You, J. Kim, D. Seong, and Y. Shin, Thin Solid Films **518**, 6694 (2010).
[41]S. Ashida, C. Lee, and M. Lieberman, J. Vac. Sci. Technol. A **13**, 2498 (1995).
[42]M. H. Lee and C. W. Chung, Phys. Plasmas **12**, 073501 (2005b).
[43]V. Godyak, *Soviet Radio Frequency Discharge Research* (Delphic Associates, Falls Church, 1986).
[44]P. Miller, G. Hebner, K. Greenberg, and P. Pochan, J. Res. Natl. Inst. Stand. Technol. **100**, 427 (1995).
[45]M. Schulze, A. Yanguas-Gil, A. Keudell, and P. Awakowicz, J. Phys. D: Appl. Phys. **41**, 065206 (2008).
[46]Y. Lee and C. Chung, J. Appl. Phys. **109**, 013306 (2011).